Self-Assembly

DOI: 10.1002/anie.201003302

Unprecedented Molecular Architectures by the Controlled Self-Assembly of a β-Peptide Foldamer**

*Sunbum Kwon, Aram Jeon, Sung Hyun Yoo, Im Sik Chung, and Hee-Seung Lee**

Nature utilizes the self-assembly of monomeric units by multiple noncovalent interactions for the construction of complex functional systems.[1] In recent decades, a variety of peptide-based scaffolds, which range from simple aromatic dipeptides to small protein fragments, have been studied in order to understand the underlying mechanism and mimic this process to create artificial nano- and microstructures.[2–6] Because of the intrinsic large conformational flexibility of short-length peptides, amphiphilic,[7,8] or cyclic[9] scaffolds have been typically employed to ensure the formation of well-defined self-assembled structures. However, in contrast to the morphologies found in inorganic nanostructures,[10] the morphologies of the peptide-based self-assembled nano- and microstructures are limited to round shapes such as spheres, tubes, and rods.[11] The ability to construct biocompatible peptide-based molecular architectures with anisotropic shapes should expand the possibilities for the design of molecular machines for diverse applications in biological and materials science.[12] Such a construction should be possible if a molecular design principle for monomeric units held together by comparable intermolecular interactions in three orthogonal directions was available; however, currently this is not the case.[13]

On the other hand, β peptides (oligomers of β amino acids) are excellent artificial peptides that can mimic protein-like secondary structures such as helices, strands, and turns.[14] The self-associating behavior of β peptides have recently been investigated,[15–18] but the construction of higher-order structures with specific morphologies is still in its infancy. Herein we report the first example of highly homogeneous, well-defined, and finite molecular architectures formed by the self-assembly of a helical β peptide in aqueous solution. The 3D shapes of the assembled nano- and microstructures can be controlled by simply changing the experimental conditions.

We used a homo-oligomer of *trans*-(*S*,*S*)-2-aminocyclopentanecarboxylic acid (ACPC) as a building block for the self-assembly. This particular β peptide resembles an α-helical peptide in terms of handedness, helical pitch, and the direction of the macrodipole moment, but is known to adopt a more stable and unique helical conformation through intramolecular 12-membered hydrogen bonding between C=O (*i*) and N–H (*i*+3) (the so-called 12-helix) in both solid state and solution, if the number of monomers exceeds approximately six residues (Figure 1a).[19] Figure 1b shows

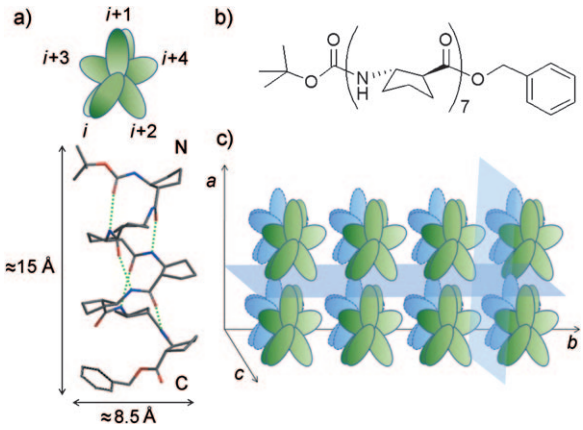

Figure 1. a) Top: cartoon showing the repeating pentad in $ACPC_7$, viewed along the helix axis; bottom: molecular model of the 12-helical *trans*-(*S*,*S*)-$ACPC_7$ oligomer, viewed perpendicular to the helix axis (intramolecular hydrogen bonds are shown as green dotted lines, hydrogen atoms are omitted for clarity); b) chemical structure of $ACPC_7$; c) schematic representation of possible molecular packing modes of $ACPC_7$ by intermolecular hydrophobic (*ac* and *bc* interfaces) and hydrogen bonding (*ab* interface) interactions during the self-assembly process in aqueous solution.

the chemical structure of the ACPC heptamer ($ACPC_7$), which is a highly hydrophobic molecule (aspect ratio ≈ 2), because the methylene units of the cyclopentane rings are displayed over the helical faces, and both the N- and C-termini are protected by a *tert*-butyloxycarbonyl (Boc) and a benzyl group, respectively. The possible modes of self-assembly of ACPC oligomers are illustrated in Figure 1c. With this simple design, $ACPC_7$ should adopt a stable right-handed 12-helix in solution. These helices in turn are likely to associate in an aqueous environment through lateral hydrophobic interactions between the helical faces as well as by

[*] S. Kwon, A. Jeon, S. H. Yoo, Prof. H.-S. Lee
Molecular-Level Interface Research Center
Department of Chemistry, KAIST
335 Gwahak-ro, Yuseong-gu, Daejeon 305-701 (Korea)
Fax: (+82) 42-350-2810
E-mail: hee-seung_lee@kaist.ac.kr
Homepage: http://hslee.kaist.ac.kr
Dr. I. S. Chung
BioNanotechnology Research Center
Korea Research Institute of Bioscience and Biotechnology (KRIBB)
52 Eoeun-Dong, Yuseong-gu, Daejeon 305-333 (Korea)

[**] This research was supported by a Basic Science Research Program of the National Research Foundation of Korea (NRF) grant funded by the Ministry of Education, Science and Technology (2009-0075849, 2009-0084449, 2010-0001953), the KAIST High Risk High Return Project (HRHRP), and a grant from the KRIBB Research Initiative Program.

Supporting information for this article is available on the WWW under http://dx.doi.org/10.1002/anie.201003302.

head-to-tail intermolecular hydrogen bonding, which could be expected based on the crystal packing modes of analogous compounds.[20]

By exposing $ACPC_7$ to an aqueous environment (solvophobic conditions), we could readily obtain a unique self-assembled structure, which was observed by scanning electron microscopy (SEM). When a solution of $ACPC_7$ in THF (200 μL, 1 mg mL^{-1}) was added to distilled water (1 mL) under vigorous stirring, a white precipitate immediately formed. The SEM image of the filtered material showed a homogeneous windmill-shaped morphology W_W (Figure 2a).

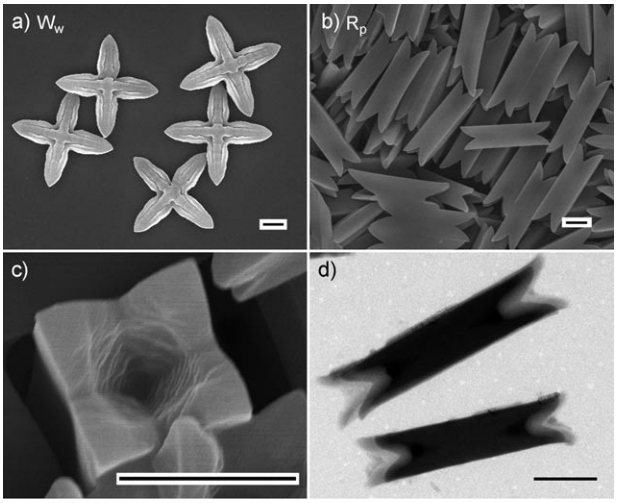

Figure 2. SEM images of the self-assembled structures of $ACPC_7$ prepared from a) distilled water (W_W) and b) an aqueous solution of P123 (0.03 g L^{-1}, R_P); c) long-axis view of R_P; d) TEM image of R_P. (Scale bars: 1 μm).

The microsized self-assembled structure (ca. 5 μm in width) has a D_{4h} symmetry with four sails, in which the dihedral angles among the sails are almost 90 degrees. The size of the uniformly shaped microstructure was controlled by tuning the heptamer concentration. Increasing the concentration of the heptamer solution resulted in larger assembled structures (e.g., a heptamer concentration of 4 mg mL^{-1} resulted in structures with widths of ca. 17 μm) in which the unique morphology was maintained (Figure S2 in the Supporting Information). Interestingly, a dramatic morphological change in the self-assembled structure obtained from the same molecule was observed when we carried out a self-assembly experiment in the presence of the nonionic surfactant P123 ((ethylene glycol)$_{20}$-(propylene glycol)$_{70}$-(ethylene glycol)$_{20}$) that has been used previously for the shape control of organic and inorganic nanostructures.[21,22] The SEM image showed that the self-assembly of $ACPC_7$ produced the rodlike 3D structure R_P (Figure 2b), which is completely different from W_W. The morphology of R_P can be described as a square rod, but in contrast to conventional rods, it has salient features: it is sharp-edged and crowned with four apexes at both ends (Figure 2c). The rod is not perfectly tubular as can be seen from the TEM image (Figure 2d). The cross-section of the rod is not perfectly square with D_{4h} symmetry as the faces of the rods are slightly tapered. This unprecedented morphology that has not been observed for any other organic building blocks is well-defined and remarkably monodisperse in size as well as in shape. This is the first molecular female joint in nano- and microscale assembly, which was not expected to be achievable by the bottom-up approach.

Self-assembly of the β peptide heptamer, which was monitored by SEM (Figure 3a–d), was carried out at different P123 concentrations. The stepwise morphological transition in the self-assembly process from the windmill shape (W_W) to the square rod (R_P) was clearly observed, thus revealing the

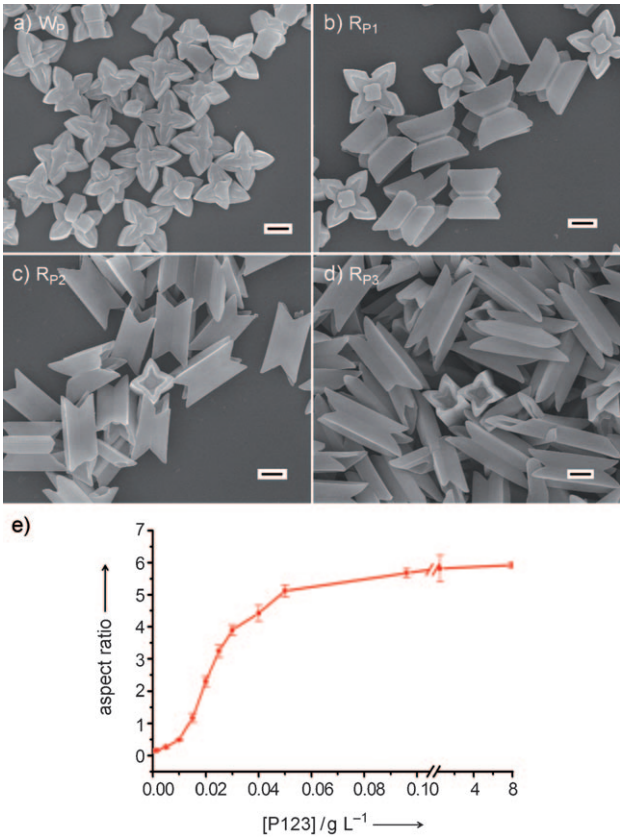

Figure 3. SEM images of the self-assembled structures of $ACPC_7$ in solutions with different P123 concentrations (scale bars: 1 μm): a) 0.01 g L^{-1} (W_P); b) 0.015 g L^{-1} (R_{P1}); c) 0.02 g L^{-1} (R_{P2}); d) 0.025 g L^{-1} (R_{P3}); e) plot of the aspect ratio (length/width) versus P123 concentration.

relationship between the morphologies of the self-assembled structures and the P123 concentration. In a highly dilute solution of P123 (0.005 g L^{-1}), the morphology of the self-assembled structures is very similar to W_W (data not shown). However, a thicker but smaller windmill shape (W_P) was obtained at 0.01 g L^{-1} (Figure 3a). Interestingly, at 0.015 g L^{-1}, the shape had grown vertically along the edges, so the convex face of W_P was inverted to be the concave face in R_{P1} (like a flower with four petals) as if it were embossed (Figure 3b). As the P123 concentration increased, R_{P1} was gradually elongated to ultimately form R_P. During the growth of the assemblies, their width became smaller and the unique shape

at both ends of the structure was further developed (Figure 2b and 3c,d).

As shown in the plot of the average aspect ratios versus the P123 concentration (Figure 3e), the longitudinal growth of the structures became dominant above a concentration of 0.015 $g L^{-1}$, which is the critical micelle concentration of P123,[23] thus suggesting that micelle formation of P123 is required in order to guide the molecular packing of $ACPC_7$ in the longitudinal direction during the self-assembly process. This analysis seemed to be reasonable because the self-assembly of $ACPC_7$ in the presence of poly(ethylene glycol) (PEG; $M_n = 950–1050$), a hydrophilic fragment of P123, could not change the structure W_W (Figure S3 in the Supporting Information). No significant change in shape was observed above a concentration of 0.03 $g L^{-1}$ of P123 up to much higher concentrations (8 $g L^{-1}$), (Figure S4 in the Supporting Information).

We examined the physical properties of the windmill shape (W_W) and the square rod (R_P) by thermogravimetric analysis (TGA), FTIR, differential scanning calorimetry (DSC), and powder X-ray diffraction (PXRD). No significant difference between W_W and R_P was observed in the TGA profiles, in which the weight loss occured above 250 °C, thus demonstrating that both β peptide self-assemblies (W_W and R_P) possess higher thermal stability than those of natural peptides; the existence of P123 in R_P could not be detected (Figure S5 in the Supporting Information). The FTIR spectra of W_W and R_P are identical, which further supports the absence of P123 in R_P (Figure S6 in the Supporting Information).

DSC analysis revealed an interesting exothermicity in the heating process (Figure 4a). We hypothesized that the exothermicity might be attributed to the lattice energy released. If both W_W and R_P structures were in energetically higher states, they would rearrange upon heating to find thermodynamically more stable molecular packing modes, thus releasing their lattice energies. W_W showed two peaks at 130 and 157 °C respectively (shown in red), while R_P has only one strong exothermic peak at 130 °C (shown in black). These data suggests that R_P is more crystalline than W_W, which is consistent with the PXRD data in Figure 4b,c. To confirm this hypothesis, the powders of W_W and R_P were heated to temperatures slightly above the temperatures that the exothermic peaks appeared at (145 °C and 180 °C for W_W, 145 °C for R_P), and were then re-examined by PXRD (Figure S7 in the Supporting Information). We found that both heat-treated samples gave almost identical well-defined PXRD patterns, which are also very similar to that of untreated R_P except for the peak sharpness and the intensities. This evidence allowed us to explain why we observed the unusual exothermic behaviors of W_W and R_P in DSC analysis, and to obtain an insight into the influence of P123 on the self-assembly process.

The P123 additive plays an important role in the crystal packing of $ACPC_7$ and is closely related to longitudinal growth in the self-assembly process. A comparison of the PXRD patterns of W_W (Figure 4b) and R_P (Figure 4c) led us to conclude that the peaks labeled with ● and ▼ are closely related to the molecular packing mode in the longitudinal direction, while the peaks labeled with ● and ■ correspond to the packing in the plane that encompasses the windmill shape. Judging from the peak intensity changes, the packing mode for the peak ■ was dominant in pure water, but was selectively inhibited by P123, thus suggesting that P123 preferentially induced the thermodynamically more stable packing modes for the peaks ● and ▼. This seems to be the reason why we observed one peak in the DSC profile of R_P.

Based on all the experimental evidence, we propose a mechanism for the self-assembly of hydrophobic β peptide $ACPC_7$ in aqueous solution (Figure 5). At the early stage of the self-assembly process, a nucleus, presumably in the form of an oligomeric $ACPC_7$ bundle, will be instantaneously generated. In the absence of P123, the subsequent crystal growth on the nuclei will occur through hydrophobic and head-to-tail hydrogen bonding interactions. Because of the limited number of molecular packing modes that result from the intrinsic conformational rigidity, the 12-helical β peptide self-assembles to give the unique windmill shape W_W. In the

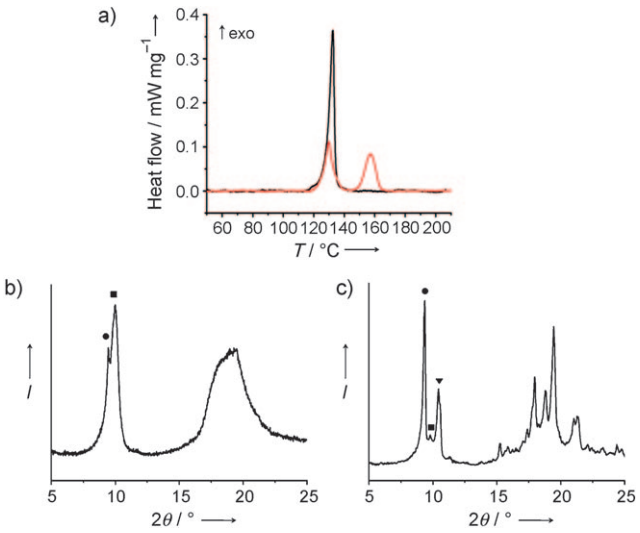

Figure 4. a) DSC profiles (overlapped) of W_W (red) and R_P (black). PXRD patterns of b) W_W and c) R_P; the *d* spacings corresponding to the peaks denoted by the symbols ●, ■, ▼ are 9.456 Å, 9.04 Å and 8.475 Å, respectively.

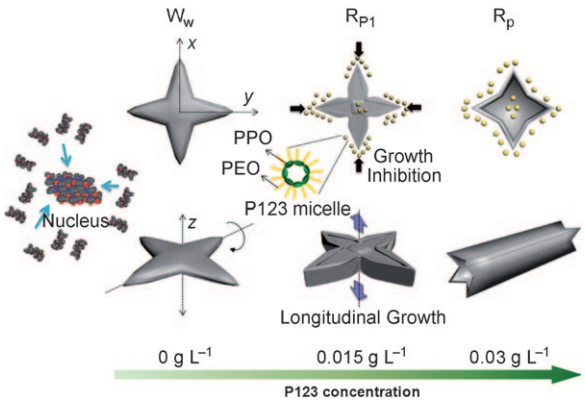

Figure 5. Proposed mechanism for the self-assembly of $ACPC_7$ in aqueous solution.

presence of P123, however, P123 micelles surround the windmill-shaped entities at an early stage of the self-assembly process and suppress the growth rate in the *x* and *y* directions, thereby rapidly increasing the growth rate in the *z* direction to give the square rod R_P. The resulting structural anisotropy of the assembly R_P should be derived from the functional anisotropy (hydrophobic and hydrophilic nature) of the assembly W_W. P123 selectively recognizes this functional anisotropy, thus resulting in the *z*-directional growth. The unique morphology developed at both ends of R_P seems to be attributable to the concentration gradient of $ACPC_7$ monomers. Molecular packing occurs from the edges of the initially formed self-assembled structures.[24] As the assembly grows along the *z* direction, the initial difference in growth rate between the inside and the outside of the rod will become more pronounced, which results in the formation of the conically shaped cavities at the final stage. It is worth noting that the role of the P123 micelles in the β peptide self-assembly process resembles that of molecular chaperones in the protein folding process in biological systems.[25] In the self-assembly process, P123 micelles help to find an energetically more favorable pathway over others and thus influence the final outcome.

In summary, we have shown the self-assembly of a 12-helical β peptide, which has a unique helical secondary structure that is not encountered in natural systems. Because of its rigid and unique conformational features in solution, the short β peptide made it possible to generate unprecedented 3D morphologies that have not been obtained from any other molecular building block. To the best of our knowledge, this is the first example of highly homogeneous, well-defined, and finite molecular architectures from a peptidic scaffold that is neither cyclic nor amphipilic. In addition, the 3D shapes could be controlled reproducibly. We believe that our results will provide a new route for the creation of diverse (chiral) functional molecular complexes as well as give an insight into the underlying mechanism of self-association of natural counterparts.

Experimental Section

Materials: All chemicals for the preparation of the peptide heptamer were purchased from Sigma Aldrich, Acros, Junsei, and TCI, and were used without further purification. High purity water was generated by a Milli-Q apparatus (Millipore). The synthesis of the heptamer is described in the Supporting Information.

Self-assembly: A solution of $ACPC_7$ in THF (200 μL, 1 mg mL^{-1}) was added to aqueous solutions of P123 of various concentrations (1 mL; 0–8 g L^{-1}) at room temperature. A white precipitate was observed after 3 min of vigorous stirring, the mixtures were then stabilized for 3 h. After washing with distilled water to remove any residual surfactants and THF, the obtained powders were dispersed in a small amount of distilled water (20 μL).

Characterization: The previously prepared dispersion of the assemblies was transferred to a Si(100) wafer (or a copper grid) and dried under air. SEM images were obtained by using a field-emission scanning electron microscope (FE-SEM, Hitachi S-4800, Japan) at an acceleration voltage of 10 kV after Pt coating (SCD 050 platinum evaporator, Bal-tec, Germany). TEM images were obtained by using a FE-TEM (Tecnai G2 F30, Philips). TGA and DSC were carried out by using a TG 209 F3 and a DSC 204 F1, respectively, with an increase in temperature of 10 °C min^{-1} (NETZSCH, Germany). PXRD patterns were obtained from a multi-purpose attachment X-ray diffractometer (Rigaku, D/Max-2500) equipped with a pyrolytic graphite (002) monochromator. Characteristic $Cu_{K\alpha}$ radiation was used as an incident beam ($\lambda = 1.54178$ Å) and the diffraction patterns were scanned over 2θ values ranging from 2° up to 35° in increments of 0.02° at room temperature. The circular dichroism signal was measured by a Jasco-815 spectrometer (Jasco. Inc., Japan) by using methanolic solutions of $ACPC_7$, sample cells with a path length of 1 mm were used. Infrared spectra of powders of $ACPC_7$ were obtained by using an ALPHA FTIR spectrometer ATR module (Bruker optics, USA).

Received: May 31, 2010
Published online: August 23, 2010

Keywords: aggregation · molecular architectures · nanostructures · peptides · self-assembly

[1] G. M. Whitesides, B. Grzybowski, *Science* **2002**, *295*, 2418 – 2421.
[2] a) A. M. Smith, R. V. Ulijn, *Chem. Soc. Rev.* **2008**, *37*, 664 – 675; b) I. Cherny, E. Gazit, *Angew. Chem.* **2008**, *120*, 4128 – 4136; *Angew. Chem. Int. Ed.* **2008**, *47*, 4062 – 4069.
[3] M. Reches, E. Gazit, *Science* **2003**, *300*, 625 – 627.
[4] C. H. Görbitz, *Chem. Eur. J.* **2001**, *7*, 5153 – 5159.
[5] Y. Lim, K.-S. Moon, M. Lee, *Angew. Chem.* **2009**, *121*, 1629 – 1633; *Angew. Chem. Int. Ed.* **2009**, *48*, 1601 – 1605.
[6] T. H. Han, T. Ok, J. Kim, D. O. Shin, H. Ihee, H.-S. Lee, S. O. Kim, *Small* **2010**, *6*, 945 – 951.
[7] S. Zhang, T. Holmes, C. Lockshin, A. Rich, *Proc. Natl. Acad. Sci. USA* **1993**, *90*, 3334 – 3338.
[8] J. D. Hartgerink, E. Beniash, S. I. Stupp, *Science* **2001**, *294*, 1684 – 1688.
[9] M. R. Ghadiri, J. R. Granja, R. A. Milligan, D. E. McRee, N. Khazanovich, *Nature* **1993**, *366*, 324 – 327.
[10] a) C. Burda, X. Chen, R. Narayanan, M. A. El-Sayed, *Chem. Rev.* **2005**, *105*, 1025 – 1102; b) Y. Xia, Y. Xiong, B. Lim, S. E. Skrabalak, *Angew. Chem.* **2009**, *121*, 62 – 108; *Angew. Chem. Int. Ed.* **2009**, *48*, 60 – 103; c) N. A. J. M. Sommerdijk, G. de With, *Chem. Rev.* **2008**, *108*, 4499 – 4550.
[11] a) X. Gao, H. Matsui, *Adv. Mater.* **2005**, *17*, 2037 – 2050; b) Y.-b. Lim, K.-S. Moon, M. Lee, *Chem. Soc. Rev.* **2009**, *38*, 925 – 934.
[12] a) N. A. Peppas, R. Langer, *Science* **1994**, *263*, 1715 – 1720; b) R. Langer, D. A. Tirrell, *Nature* **2004**, *428*, 487 – 492; c) S. Mitragotri, J. Lahann, *Nat. Mater.* **2009**, *8*, 15 – 23.
[13] G. R. Desiraju, *Angew. Chem.* **2007**, *119*, 8492 – 8508; *Angew. Chem. Int. Ed.* **2007**, *46*, 8342 – 8356.
[14] a) R. P. Cheng, S. H. Gellman, W. F. DeGrado, *Chem. Rev.* **2001**, *101*, 3219 – 3232; b) D. Seebach, A. K. Beck, D. J. Bierbaum, *Chem. Biodiversity* **2004**, *1*, 1111 – 1239; c) C. M. Goodman, S. Choi, S. Shandler, W. F. DeGrado, *Nat. Chem. Biol.* **2007**, *3*, 252 – 262.
[15] a) T. D. Clark, L. K. Buehler, M. R. Ghadiri, *J. Am. Chem. Soc.* **1998**, *120*, 651 – 656.
[16] a) T. L. Raguse, J. R. Lai, P. R. Leplae, S. H. Gellman, *Org. Lett.* **2001**, *3*, 3963 – 3966; b) W. C. Pomerantz, V. M. Yuwono, C. L. Pizzey, J. D. Hartgerink, N. L. Abbott, S. H. Gellman, *Angew. Chem.* **2008**, *120*, 1261 – 1264; *Angew. Chem. Int. Ed.* **2008**, *47*, 1241 – 1244; c) C. L. Pizzey, W. C. Pomerantz, B.-J. Sung, V. M. Yuwono, S. H. Gellman, J. D. Hartgerink, A. Yethiraj, N. L. Abbott, *J. Chem. Phys.* **2008**, *129*, 095103.
[17] a) T. A. Martinek, A. Hetényi, L. Fülöp, I. M. Mándity, G. K. Tóth, I. Dékány, F. Fülöp, *Angew. Chem.* **2006**, *118*, 2456 – 2460; *Angew. Chem. Int. Ed.* **2006**, *45*, 2396 – 2400; b) A. Hetényi, I. M. Mándity, T. A. Martinek, G. K. Tóth, F. Fülöp, *J. Am. Chem. Soc.* **2005**, *127*, 547 – 553; c) T. A. Martinek, I. M. Mándity, L. Fülöp,

G. K. Tóth, E. Vass, M. Hollósi, E. Forró, F. Fülöp, *J. Am. Chem. Soc.* **2006**, *128*, 13539 – 13544.

[18] a) D. S. Daniels, E. J. Petersson, J. X. Qiu, A. Schepartz, *J. Am. Chem. Soc.* **2007**, *129*, 1532 – 1533; b) J. X. Qiu, E. J. Petersson, E. E. Matthews, A. Schepartz, *J. Am. Chem. Soc.* **2006**, *128*, 11338 – 11339; c) J. L. Goodman, E. J. Petersson, D. S. Daniels, J. X. Qiu, A. Schepartz, *J. Am. Chem. Soc.* **2007**, *129*, 14746 – 14751.

[19] a) D. H. Appella, L. A. Christianson, D. A. Klein, D. R. Powell, X. Huang, J. J. Barchi, S. H. Gellman, *Nature* **1997**, *387*, 381 – 384; b) E. A. Porter, X. Wang, H.-S. Lee, B. Weisblum, S. H. Gellman, *Nature* **2000**, *404*, 565; c) J. J. Barchi, X. Huang, D. H. Appella, L. A. Christianson, S. R. Durell, S. H. Gellman, *J. Am. Chem. Soc.* **2000**, *122*, 2711 – 2718.

[20] D. H. Appella, L. A. Christianson, D. A. Klein, M. R. Richards, D. R. Powell, S. H. Gellman, *J. Am. Chem. Soc.* **1999**, *121*, 7574 – 7581.

[21] S. J. Lee, J. T. Hupp, S. T. Nguyen, *J. Am. Chem. Soc.* **2008**, *130*, 9632 – 9633.

[22] X. Zhang, C. Dong, J. A. Zapien, S. Ismathullakhan, Z. Kang, J. Jie, X. Zhang, J. C. Chang, C.-S. Lee, S.-T. Lee, *Angew. Chem.* **2009**, *121*, 9285 – 9287; *Angew. Chem. Int. Ed.* **2009**, *48*, 9121 – 9123.

[23] a) G. Wanka, H. Hoffmann, W. Ulbricht, *Colloid Polym. Sci.* **1990**, *268*, 101 – 117; b) G. Wanka, H. Hoffmann, W. Ulbricht, *Macromolecules* **1994**, *27*, 4145 – 4159.

[24] a) G. C. Krueger, C. W. Miller, *J. Chem. Phys.* **1953**, *21*, 2018 – 2023; b) S. M. Yoon, I.-C. Hwang, K. S. Kim, H. C. Choi, *Angew. Chem.* **2009**, *121*, 2544 – 2547; *Angew. Chem. Int. Ed.* **2009**, *48*, 2506 – 2509.

[25] a) A. L. Horwich, G. W. Farr, W. A. Fenton, *Chem. Rev.* **2006**, *106*, 1917 – 1930; b) D. Rozema, S. H. Gellman, *J. Am. Chem. Soc.* **1995**, *117*, 2373 – 2374.

